ARTICLES

Journal of Semiconductors
(2019) 40, 072901
doi: 10.1088/1674-4926/40/7/072901

Electrically driven uniaxial stress device for tuning *in situ* semiconductor quantum dot symmetry and exciton emission in cryostat

Hao Chen[1, 2], Xiuming Dou[1, 2, †], Kun Ding[1], and Baoquan Sun[1, 2, †]

[1]State Key Laboratory for Superlattices and Microstructures, Institute of Semiconductors, Chinese Academy of Sciences, Beijing 100083, China
[2]College of Materials Science and Optoelectronic Technology, University of Chinese Academy of Sciences, Beijing 100049, China

Abstract: Uniaxial stress is a powerful tool for tuning exciton emitting wavelength, polarization, fine-structure splitting (FSS), and the symmetry of quantum dots (QDs). Here, we present a technique for applying uniaxial stress, which enables us *in situ* to tune exciton optical properties at low temperature down to 15 K with high tuning precision. The design and operation of the device are described in detail. This technique provides a simple and convenient approach to tune QD structural symmetry, exciton energy and biexciton binding energy. It can be utilized for generating entangled and indistinguishable photons. Moreover, this device can be employed for tuning optical properties of thin film materials at low temperature.

Key words: uniaxial stress; electrically driven device; low temperature; quantum dots; thin film materials

Citation: H Chen, X M Dou, K Ding , and B Q Sun, Electrically driven uniaxial stress device for tuning *in situ* semiconductor quantum dot symmetry and exciton emission in cryostat[J]. *J. Semicond.*, 2019, 40(7), 072901. http://doi.org/10.1088/1674-4926/40/7/072901

1. Introduction

Single photon and entangled photon pairs emitters on demand are a major building block for quantum computation and communication[1–3]. Self-assembled semiconductor quantum dots (QDs) combine atomic spectral properties and solid-state extensibility, which are considered to be the most promising single photon and entangled photon sources[4–7]. However, exciton states of QDs usually split into two levels with a fine-structure splitting (FSS) of tens of μeV, which is due to a lack of rotational symmetry in QD growth plane. Note that several techniques of epitaxial growth of QDs, such as doping and pattern substrate growth, are employed for trying to remove QD FSS. However, it is still difficult to obtain the QDs with a FSS ~ 0. Over the past few decades, techniques of tuning QD optical properties have been developed[8], such as varying temperature, applied electrical field[9, 10], magnetic field[11], hydrostatic pressure[12], uniaxial and biaxial stress[13, 14]. Among these tuning techniques, tuning temperature will induce spectral broadening; electric-induced shift of the emission peak is on the order of 1 nm for InAs/GaAs QDs; magnetic fields may further lead to level splitting; applied hydrostatic pressure can tune QD emission wavelength up to 160 nm. However, reversible tuning of applied pressure may be difficult. In recent years, it was reported that a wavelength-tunable entangled photon emitter is realized by employing a piezoelectric motivator, such as a type of piezoelectric crystal named PMN-PT[13, 15–17]. Another simple and convenient method of applied uniaxial stress, such as two-point bending apparatus[18, 19], is usually used to tune band edge emission of two-dimensional thin film materials, which is often employed at room temperature. Here, we report on an applied uniaxial stress method with controllable, convenient, and large tuning scale operated in cryostat.

Correspondence to: X M Dou, xmdou04@semi.ac.cn; B Q Sun, bqsun@semi.ac.cn
Received 4 MAY 2019; Revised 29 MAY 2019.

2. Experimental setup

2.1. Design of the electrically driven uniaxial stress device

In this article, we report on a technique of applied uniaxial stress on the sample at low temperature. As shown in Fig. 1(a), firstly, the sample is needed to be prepared into a thin film and transferred it onto the center of the polished metal sheet, where the sample film is absorbed on the metal sheet by van der Waals force. Two pairs of round holes on the edge of the sheet along with diagonal line are used to fix the string and stretch the metal sheet. In this case the uniaxial stress can be applied in four directions of the sample. Second, the metal sheet is fixed on the scaffold with the help of a wedge and two screws, as shown in Fig. 1(b). A hook is used to hook two strings. The other end of the hook is connected to a slider, forming a system similar to a fixed pulley. The piezoelectric motor connected with the slider is employed to bend metal sheet and apply uniaxial stress on the sample. In addition, in order to keep piezoelectric motor working normally, we fix it on the side wall of the cryostat for its working at room temperature. In this case, the designed device has an advantage of the sample at low temperature and piezoelectric motor at room temperature, separately.

2.2. Temperature calibration

Note that the lowest temperature of the platform temperature of cryostat displays 4 K in our cryostat. However, this temperature is not an actual temperature of the sample on the device. To calibrate the sample temperature, small particles of

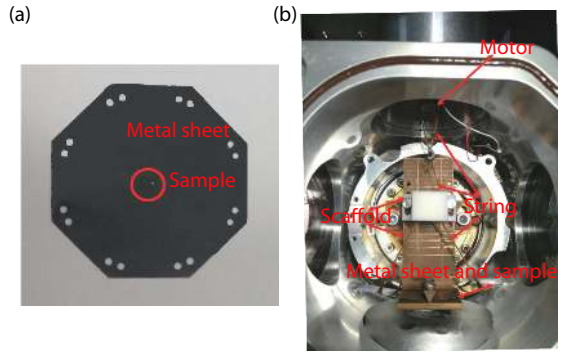

Fig. 1. (Color online) (a) Photograph of a polished metal sheet with a sample on the center, where metal sheet as a flexible substrate of absorbed sample. (b) Photograph of the electrically driven uniaxial stress device fixed on the cold chamber of cryostat.

Ruby are adhered to the metal sheet. The exact temperature of the sample on the metal sheet can be obtained by measuring the intensity ratio R_2/R_1 of the Ruby photoluminescence (PL) peaks R_2 and R_1. A small piece of Ruby is stuck on the platform of the cryostat, then the intensity ratio R_2/R_1 as a function of temperature is obtained, shown in Fig. 2(a). Fig. 2(b) shows the PL spectrum of ruby on the metal sheet at a temperature of about 15 K. It is found that with applying tension or release stress, PL peak wavelength of ruby remains to be unchanged, indicating that the temperature of the metal sheet is stable.

2.3. Stress calibration

Note that uniaxial tensile stress-dependent PL peak shift of GaAs has been reported, corresponding PL peak red shift at a rate of 33 μeV/MPa[20, 21]. Next based on the red shift rate of

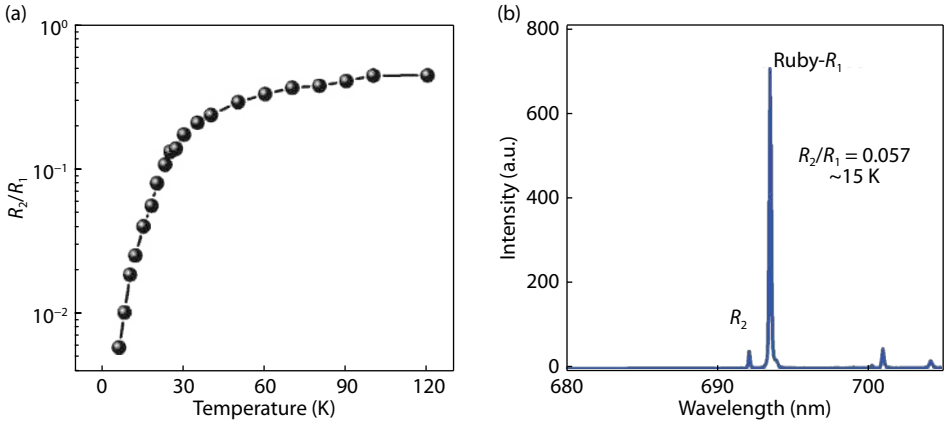

Fig. 2. (Color online) (a) PL intensity ratio R_2/R_1 of ruby as a function of temperature. (b) Ruby PL spectrum at 15 K corresponding a ratio of PL intensity of R_2 and R_1.

GaAs bandgap PL, we can calibrate the applied stress value on the InAs/GaAs QDs by measuring GaAs and QD PL spectra at the same time. In the experiment, we first obtain GaAs PL peak red shift as a function of electric motor steps, as shown in Fig. 3(a). Then the corresponding stress values, based on a rate of 33 μeV/MPa, are indicated. Fig. 3(b) summaries a red shift of GaAs peak energy with applying stress for tensile process (black solid squares) and release process (red solid circles). Such a reversible tuning process presents that the design strain device can be employed at low temperature with a simple and convenient strain tuning.

3. Several applications of the uniaxial stress device

In the following we will measure the PL spectral shifts of exciton (X), biexciton (XX), and charged (X*) exciton emissions, as well as charged exciton decay time and exciton FSS of InAs/GaAs QDs by using developed uniaxial stress tuning device at 15 K. In addition, band edge PL shift of two-dimensional thin film materials is also measured.

3.1. In situ tuning exciton, biexciton and charged exciton emissions

The studied InAs/GaAs QD samples were grown on a (001) GaAs substrate by molecular beam epitaxy (MBE). It consists of a 200 nm GaAs buffer layer, a 100 nm AlAs sacrificial layer, a 30 nm GaAs layer, a InAs QD layer, and a 100 nm GaAs cap layer. After etching away the AlAs sacrificed layer, we transferred a thin film with a thickness of 130 nm GaAs containing InAs QDs onto the polished metal sheet (see Fig. 1(a)), while the sample's (110) crystal orientation of GaAs at zero stress was aligned along one of the applied uniaxial stress direction carefully.

The QDs was excited by a λ = 640 nm semiconductor laser. The excitation laser was focused to a spot with a diameter of ~2 μm on the sample using a microscope objective (NA: 0.45). The PL was collected using the same objective, and measured using a 0.5 m focal length monochrometer equipped with a silicon charge-coupled device.

Fig. 4(a) presents the measured PL spectra of X, XX and X* at 15 K under different uniaxial stresses. It can be seen that all the exciton PL peaks show a kind of red shift as the stress increases from 0 to 717.6 MPa. The corresponding red shift of PL peak wavelength is approximately 7 nm, which can be tuned *in situ* at 15 K continuously. We also found that the PL intensities show a decrease with increasing stress. Fig. 4(b) shows a plot of PL peak energies as function of applied stress. By linearly fit to data, the obtained stress coefficients for X, XX and X* are –20.26, –18.93 and –20.19 μeV/MPa, respectively.

3.2. Radiation lifetime and FSS under applied stress

The QD PL decay curve is measured by using silicon avalanche photodiode (APD) and time-correlated single photon counting (TCSPC) setup with an instrument response time of ~ 300 ps at 15 K.

Note that two non-degenerates bright X emissions correspond to two mutually perpendicular linearly polarized photon

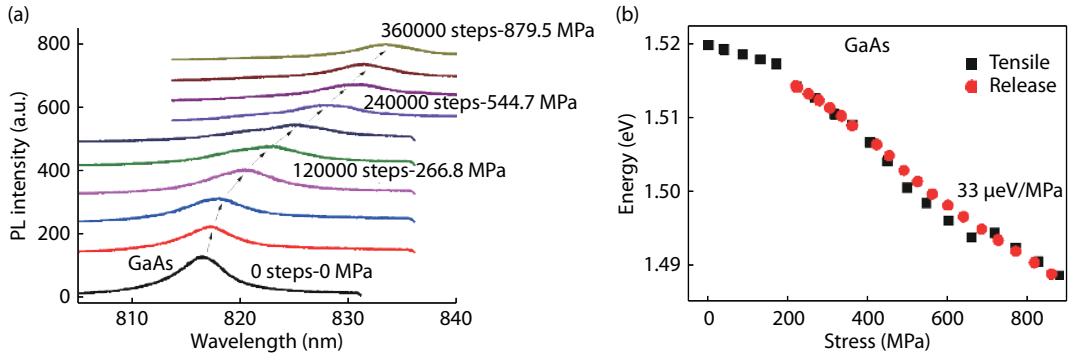

Fig. 3. (Color online) (a) Stress-dependent spectra of GaAs at 15 K, measured for applied uniaxial tensile stress from zero to 879.5 MPa. (b) PL peak energy as a function of tensile (black solid squares) and release (red solid circles) stresses, respectively.

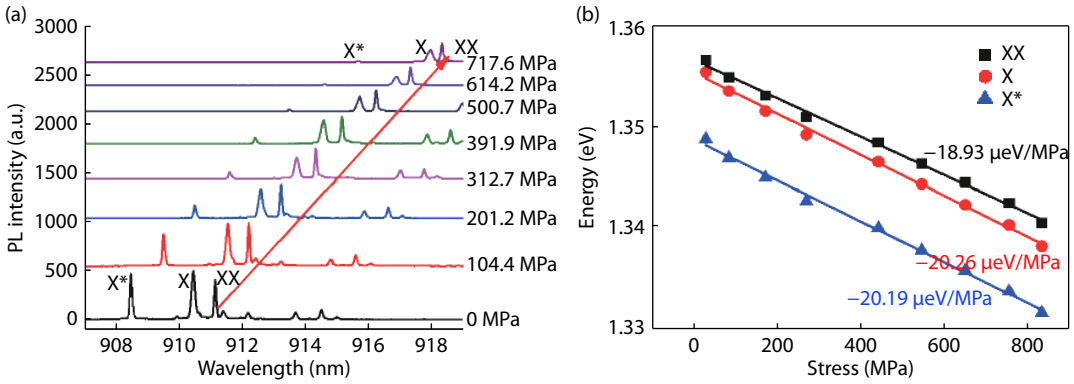

Fig. 4. (Color online) (a) PL spectra for X*, X and XX in QD measured under the tensile stress of 0, 104.4, 201.2, 321.7, 391.9, 500.7, 614.2 and 717.6 MPa, respectively. (b) The obtained stress coefficients for X*, X and XX are −20.19, −20.26 and −18.93 μeV/MPa, respectively.

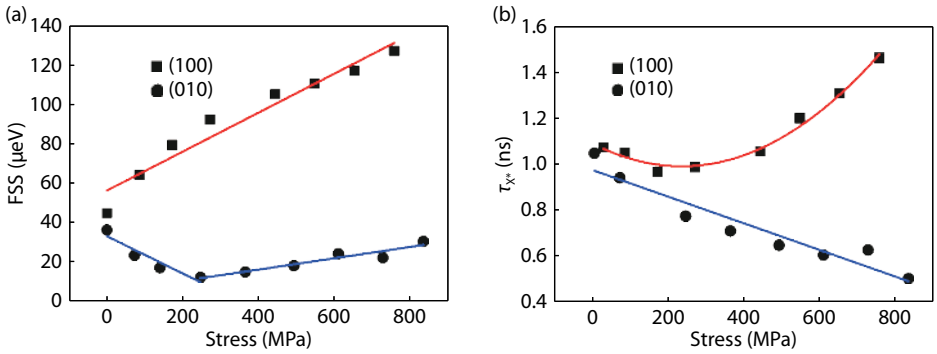

Fig. 5. (Color online) (a) FSS change of the exciton in single QD as a function of strain applied along (100) and (010) directions, respectively. (b) Charged exciton decay times of single QD as a function of strain applied along (100) and (010) directions, respectively.

emissions[22, 23]. One of the polarized planes of the linearly polarized light follows the (100) direction and the other is along the (010). Thus in the experiments, FSS and decay time of X* are measured under applied stress along (100) and (010) directions. The corresponding results are showed in Fig. 5. It can be seen from Fig. 5(a) that FSS increases as the stress is applied along (100), implying further deterioration of rotational symmetry of QDs. By contrast, FSS decreases firstly and then increases again as the stress is applied along (010). In this case, the smallest FSS can be reached. In addition, the decay time of X* are also measured for applied stress along (100) and (010) directions, as shown in Fig. 5(b). It clearly shown that the stress responses of the decay time of X* demonstrate completely different behavior. The physical mechanism needs to be further studied.

3.3. Realizing the entanglement condition of time reordering

An alternative proposal to generate entangled photon pairs from QDs, without any fundamental requirements on the FSS to be smaller (instead, a larger FSS may be better) than the radiative line width, is the so-called time reordering scheme[24]. However, this scheme requires the emission wavelengths of X and XX to be the same. It is found in Fig. 4 that both X and XX emission wavelengths show red shift with increasing the tensile stress and the red shift rate of X emission line is faster than that of XX emission lime, which provides a controllable strategy to tune the biexciton binding energy E_B(XX) to be zero. As shown in Figs. 6(b) and 6(d), PL spectra of the horizontally (red lines, Hx, Hxx) and vertically (black lines, Vx, Vxx) polarized components of exciton and biexciton PL overlap

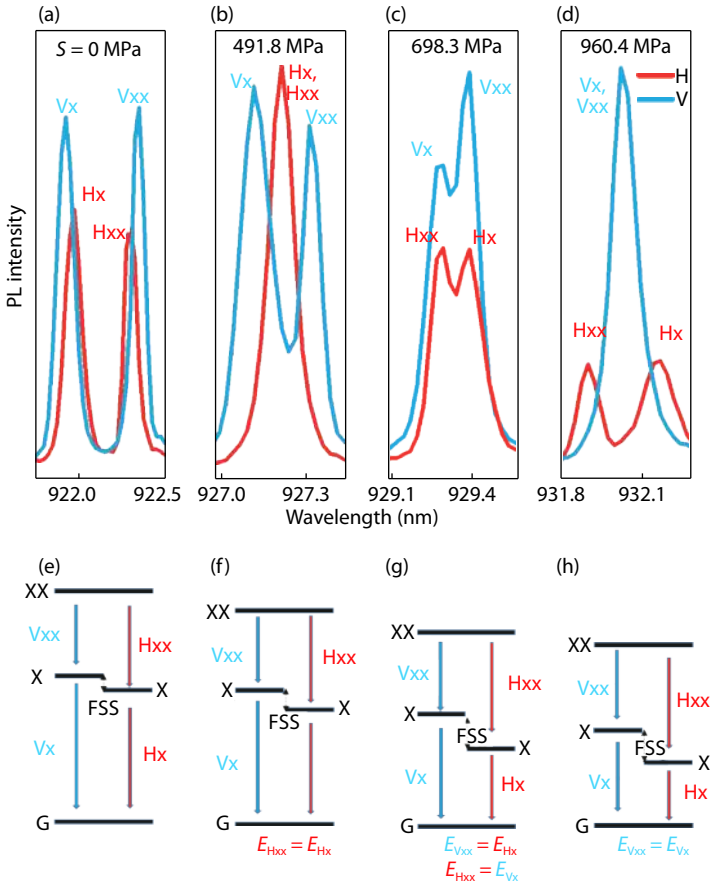

Fig. 6. (Color online) (a)–(d) Stress-dependent spectra of single QD at 15 K. As shown in (b) and (d), PL spectra of the horizontal (red lines) and vertical (black lines) polarized components of exciton and biexciton overlap at the stresses of 491.8 and 960.4 MPa, respectively. At 698.3 MPa as shown in (c), across generation color coincidence for XX and X transition energies is achieved. (e)–(h) Level schemes showing the XX-X cascade emissions accordingly.

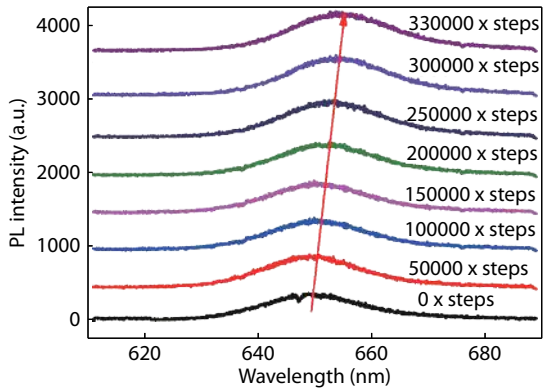

Fig. 7. (Color online) Stress-dependent PL spectra of monolayer MoS_2 at 15 K, corresponding motor precession from 0 to 330 000 steps.

each other, i.e., $E_B(XX) = 0$ corresponding to the horizontal and vertical components at the stresses of 491.8 and 960.4 MPa, respectively. In this case, XX-X cascade emission energies meet the conditions of $E_{Hxx} = E_{Hx}$ and $E_{Vxx} = E_{Vx}$, respectively, as shown in Fig. 6(f) and 6(h). Between these two applied stresses, at 698.3 MPa as shown in Fig. 6(c), XX-X cascade emission energies meet the conditions of $E_{Vxx} = E_{Hx}$ and $E_{Hxx} = E_{Vx}$, as schematically indicated in Fig. 6(g). In this case, across generation color coincidence for XX and X transition energies is achieved, realizing the condition of time reordering scheme for generation of entanglement of XX-X cascade emissions. The related entanglement experiment will be completed in the future.

3.4. Tuning PL spectra of thin film materials

The uniaxial stress device can also be used to tune band edge PL of two-dimensional thin film materials at low temperature. Here monolayer MoS_2 is chosen for its stress-independent PL measurements. Monolayer MoS_2 is first exfoliated onto a Si/SiO_2 substrate. Then the target monolayer is transferred into a polished metal sheet using poly(methyl methacrylate) (PMMA) as the transfer medium. After transferring, the PMMA is removed. Fig. 7 show the measured PL spectra under different stresses at 15 K, indicating PL peak red shift as increasing stress.

4. Summary

In summary, we have presented a technique for electrically driven uniaxial stress device which can be employed at low temperature. It enables us *in situ* tune exciton optical properties at 15 K with a single and convenient way. For the typical applications, stress-tuning optical properties of single InAs/GaAs QDs and band edge PL of monolayer MoS_2 are presented.

Acknowledgements

This work was supported by the National Key Research and Development Program of China (Grant No. 2016YFA0301202) and the National Natural Science Foundation of China (Grant No. 61674135).

References

[1] Stevenson R M, Hudson A J, Bennett A J, et al. Evolution of entanglement between distinguishable light states. Phys Rev Lett, 2008, 101(17), 170501

[2] Gao W B, Fallahi P, Togan E, et al. Observation of entanglement between a quantum dot spin and a single photon. Nature, 2012, 491(7424), 426

[3] Lodahl P, Mahmoodian S, Stobbe S. Interfacing single photons and single quantum dots with photonic nanostructures. Rev Mod Phys, 2015, 87, 347

[4] Aharonovich I, Englund D, Toth M. Solid-state single-photon emitters. Nat Photonics, 2016, 10, 631

[5] Delteil A, Sun Z, Gao W B, et al. Generation of heralded entanglement between distant hole spins. Nat Phys, 2016, 12, 218

[6] Senellart P, Solomon G, White A. High-performance semiconductor quantum-dot single-photon sources. Nat Nanotechnol, 2017, 12(11), 1026

[7] Wang H, Hu H, Chung T H, et al. On-demand semiconductor source of entangled photons which simultaneously has high fidelity, efficiency, and indistinguishability. Phys Rev Lett, 2019, 122(11), 113602

[8] Plumhof J D, Trotta R, Rastelli A, et al. Experimental methods of post-growth tuning of the excitonic fine structure splitting in semiconductor quantum dots. Nanoscale Res Lett, 2012, 7(1), 336

[9] Bennett A J, Pooley M A, Stevenson R M, et al. Electric-field-induced coherent coupling of the exciton states in a single quantum dot. Nat Phys, 2010, 6(12), 947

[10] Ghali M, Ohtani K, Ohno Y, et al. Generation and control of polarization-entangled photons from GaAs island quantum dots by an electric field. Nat Commun, 2012, 3, 661

[11] Trotta R, Zallo E, Ortix C, et al. Universal recovery of the energy-level degeneracy of bright excitons in InGaAs quantum dots without a structure symmetry. Phys Rev Lett, 2012, 109(14), 147401

[12] Wu X F, Wei H, Dou X M, et al. In situ tuning biexciton antibinding-binding transition and fine-structure splitting through hydrostatic pressure in single InGaAs quantum dots. Europhys Lett, 2014, 107(2), 27008

[13] Wang J, Gong M, Guo G C, et al. Eliminating the fine structure splitting of excitons in self-assembled InAs/GaAs quantum dots via combined stresses. Appl Phys Lett, 2012, 101(6), 2513

[14] Dou X, Sun B, Wang B, et al. Photoluminescence energy and fine structure splitting in single quantum dots by uniaxial stress. Chin Phys Lett, 2008, 25(3), 1120

[15] Keil R, Zopf M, Chen Y, et al. Solid-state ensemble of highly entangled photon sources at rubidium atomic transitions. Nat Commun, 2017, 8, 15501

[16] Zhang J, Wildmann J S, Ding F, et al. High yield and ultrafast sources of electrically triggered entangled-photon pairs based on strain-tunable quantum dots. Nat Commun, 2015, 6, 10067

[17] Ding F, Singh R, Plumhof J D, et al. Tuning the exciton binding energies in single self-assembled InGaAs/GaAs quantum dots by piezoelectric-induced biaxial stress. Phys Rev Lett, 2010, 104(6), 067405

[18] Desai S B, Seol G, Kang J S, et al. Strain-induced indirect to direct bandgap transition in multi layer WSe_2. Nano Lett, 2014, 14(8), 4592

[19] Conley H J, Wang B, Ziegler J I, et al. Bandgap engineering of strained monolayer and bilayer MoS_2. Nano Lett, 2013, 13(8), 3626

[20] Cardona M. Piezo-electroreflectance in Ge, GaAs, and Si. Phys Rev, 1968, 172(3), 816

[21] Seidl S, Kroner M, Högele, Alexander, et al. Effect of uniaxial stress on excitons in a self-assembled quantum dot. Appl Phys Lett, 2006, 88(20), 2513

[22] Gong M, Zhang W, Guo G C, et al. exciton polarization, fine-structure splitting, and the asymmetry of quantum dots under uniaxial stress. Phys Rev Lett, 2011, 106(22), 227401

[23] Xiong W, Xu X, Luo J W, et al. fundamental intrinsic lifetimes in semiconductor self-assembled quantum dots. Phys Rev Appl, 2018, 10(4), 044009

[24] Troiani F, Tejedor C. Entangled photon pairs from a quantum-dot cascade decay: The effect of time reordering. Phys Rev B, 2008, 78(15), 155305